

Quasi-two-dimensional metallic ground state of $\text{Ca}_3\text{Ru}_2\text{O}_7$

Yoshiyuki Yoshida* and Ichiro Nagai

*Japan Society for the Promotion of Science, Chiyoda, Tokyo 102-8471, Japan and
Nanoelectronics Research Institute, AIST, Tsukuba, 305-8568, Japan*

Shin-Ichi Ikeda and Naoki Shirakawa

Nanoelectronics Research Institute, AIST, Tsukuba, 305-8568, Japan

Masashi Kosaka and Nobuo Mōri

Faculty of Science, Saitama University, Saitama, 338-8570, Japan

(Received 27 April 2004; published 24 June 2004)

We have succeeded in growing single crystals of $\text{Ca}_3\text{Ru}_2\text{O}_7$ using a floating-zone method. The temperature dependence of the electrical resistivity establishes that $\text{Ca}_3\text{Ru}_2\text{O}_7$ develops a quasi-two-dimensional metallic ground state below 30 K, from which the observed quantum oscillation derives. The temperature dependence of specific heat reveals the electronic specific-heat coefficient γ to be as small as 1.7 mJ/Ru mol K². A qualitative difference exists between the field dependences of ρ_{ab} and ρ_c . The field dependence of the resistivity at the metamagnetic transition around 6 T can be explained from the tunneling magnetoresistance.

DOI: 10.1103/PhysRevB.69.220411

PACS number(s): 75.30.Kz, 75.40.Cx, 75.50.Ee, 71.30.+h

The Ruddlesden-Popper (R-P) type ruthenates $(\text{Sr,Ca})_{n+1}\text{Ru}_n\text{O}_{3n+1}$ show a wide variety of magnetic and transport properties, making them one of the most actively studied systems in solid-state physics. Sr-based materials are all metallic, and ferromagnetic (FM) correlations play an important role for $n=2, \infty$. Single-layered Sr_2RuO_4 ($n=1$) is well known as a spin triplet superconductor with $T_c=1.5$ K.¹⁻³ Double-layered $\text{Sr}_3\text{Ru}_2\text{O}_7$ ($n=2$) shows the Fermi-liquid behavior and FM instability in the ground state,^{4,5} which relates to a lately discussed quantum criticality tuned by a magnetic field.⁶ The most three-dimensional (3D) SrRuO_3 ($n=\infty$) is an itinerant FM metal with $T_C=160$ K.^{7,8}

On the other hand, Ca-based materials show different characters compared with Sr-based ones, which reflects the smaller ionic radius of Ca^{2+} than of Sr^{2+} . This causes both a rotation and a tilting of the RuO_6 octahedra, which often affect electrical and magnetic properties. Ca_2RuO_4 exhibits a metal-insulator transition with $T_{\text{MI}}=357$ K and orders antiferromagnetically at 110 K.^{9,10} A recent study revealed that Mott insulating Ca_2RuO_4 turns into FM metal under pressure.¹¹ CaRuO_3 was once thought to be a conventional paramagnetic (PM) metal with antiferromagnetic (AFM) spin interactions, but recent studies proposed that its magnetic ground state was a nearly FM metal.^{12,13}

Among the series $(\text{Sr,Ca})_{n+1}\text{Ru}_n\text{O}_{3n+1}$, we have selected $\text{Ca}_3\text{Ru}_2\text{O}_7$ for the following reasons. $\text{Ca}_3\text{Ru}_2\text{O}_7$, which stands in the series between the metallic PM CaRuO_3 and the Mott insulating AFM Ca_2RuO_4 , is expected to show an interesting interplay between conduction and magnetism. According to the previous report on single crystals grown by a CaCl_2 -flux method, $\text{Ca}_3\text{Ru}_2\text{O}_7$ shows a metallic AFM between $T_{\text{MI}}=48$ K (the first-order metal-to-nonmetal transition) and AFM ordering (Néel) temperature, $T_N=56$ K.¹⁴ The crystal structure is a double-layered R-P type with orthorhombic symmetry and the $Bb2_1m$ space group, which has

both the rotation and tilting of RuO_6 octahedral.¹⁵ It was also reported that $\text{Ca}_3\text{Ru}_2\text{O}_7$ had a substantial electronic specific-heat coefficient, $\gamma=18.5-22$ mJ/Ru mol K², even in the insulating state, which was determined from the specific-heat measurement.^{14,16} Furthermore, they recently remarked that the Shubnikov-de Haas oscillations with a very low frequency were observed in the seemingly insulating ground state.¹⁷ Although the partial gapping of the Fermi surface, which was discussed in their previous report, may be consistent with this observation, these phenomena drive us to the question of whether an insulating state can have such a high density of states near the Fermi energy.

Recently, we have succeeded in obtaining single crystals of $\text{Ca}_3\text{Ru}_2\text{O}_7$ using a floating zone (FZ) method, which is generally expected to be purer than crystals by a flux method. In this work, we report a highly anisotropic electrical resistivity, magnetization curves with hysteresis, the anomalous field dependence of in-plane resistivity, and the very small electronic specific heat of $\text{Ca}_3\text{Ru}_2\text{O}_7$. The quantum oscillations have been actually observed in the quasi-two-dimensional (2D) metallic state.

For single-crystal growth by the FZ method, considering the fact that RuO_2 easily evaporates at high temperature, we employed a self-flux technique using a commercial FZ furnace (Crystal System, Model FZ-T-10000-H-II-P-M). The constituent phase of crystals was confirmed by x-ray diffraction patterns with $\text{CuK}\alpha$ radiation for powdered crystals, as shown in Fig. 1. We estimated lattice parameters with orthorhombic symmetry. The obtained a , b , and c lattice parameters were 5.396, 5.545, and 19.61 Å, respectively, which were consistent with the previous report.¹⁶ Although the powder prepared from crushed single crystals was still slightly oriented to the c axis, good assignments of (hkl) indices to all the peaks were obtained. We emphasize that common impurity phases (CaRuO_3 or Ca_2RuO_4) were not detected.

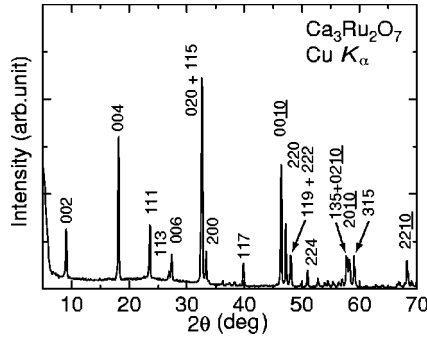


FIG. 1. X-ray diffraction patterns on powdered $\text{Ca}_3\text{Ru}_2\text{O}_7$ single crystals.

The electrical resistivity (ρ) was measured by the standard four-probe method between $T=50$ mK and 300 K and in the field up to 17 T with a superconducting magnet. The measurements of magnetic susceptibility (χ) and magnetization (M) were performed using a commercial superconducting quantum interference device magnetometer (Quantum Design, MPMS). The specific heat (C_p) measurements were carried out by a relaxation method (Quantum Design, PPMS) between 0.4 and 300 K.

Figure 2(a) shows the temperature (T) dependences of ρ for the current along the a axis (ρ_a) and the c axis (ρ_c). Considerable anisotropy between ρ_a and ρ_c is observed at all the temperatures. Above 56 K, ρ_a shows metallic behavior ($d\rho/dT > 0$), while ρ_c is nonmetallic. Both ρ_a and ρ_c de-

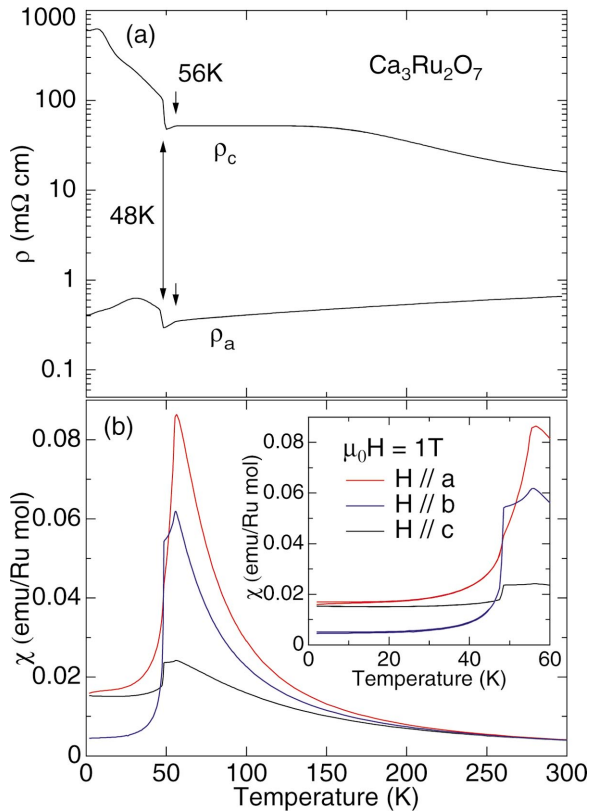


FIG. 2. (Color) The temperature dependences of (a) electrical resistivities and (b) magnetic susceptibilities of $\text{Ca}_3\text{Ru}_2\text{O}_7$.

crease slightly at 56 K on cooling and then increase discontinuously at 48 K, which agrees with the previous report.¹⁴ At 48 K, the jump of the lattice parameters was observed in a thermal contraction measurement, from which the first-order transition is evident.¹⁸ For $T < 48$ K, ρ_c is insulating, except for below 10 K, where ρ_c levels off. On the other hand, ρ_a increases from 48 to 30 K, but a metallic transport appears again below 30 K. Metallic conductivity is also observed for currents along other directions within the ab plane below 30 K. Below 20 K, ρ for the current along [110] follows T^2 -like dependence. But ρ_a and ρ_b show T -linear dependence rather than T^2 . The values for ρ_a and ρ_c at 0.2 K are 0.41 and 614 m Ω cm, respectively. The anisotropy ratio ρ_c/ρ_a varies from 25 at 300 K to 1500 at 0.2 K. These results clearly indicate that $\text{Ca}_3\text{Ru}_2\text{O}_7$ has a quasi-two-dimensional metallic ground state.

Temperature dependences of χ from 2–300 K are shown in Fig. 2(b). The magnetic field of 1 T was applied along the three principal axes. With decreasing T from 300 K, $\chi(T)$ for all directions exhibit a Curie-Weiss (C-W)-like increase. However, the deviation from the C-W law and the anisotropic behavior of $\chi(T)$ rapidly build up below 150 K and the a axis evidently becomes the easy axis. Compared with other directions, χ_c increasingly deviates from the C-W law towards T_N . We have tried to fit $\chi(T)$ to the C-W law [$\chi(T) = C/(T - \theta)$] in the PM state between 150 and 300 K. The obtained values of the effective moments and the Weiss temperatures for the a , b , and c axes are 2.74, 2.78, 2.87 μ_B and 80, 68, 50 K, respectively. These Weiss temperatures have the same sign as those of the latest report.¹⁶ However, the value for χ_c may not be significant because below 150 K, χ_c takes on a downward shift from the C-W law and ceases to diverge at a finite temperature, indicating a developing AFM correlation. The two positive values of the Weiss temperature for χ_a and χ_b imply that FM correlation predominates within the ab plane in the PM region. From 56 to 48 K, $\chi(T)$ within the ab plane decreases steeply, while the one along the c axis is almost constant. In this temperature region, the magnetic moments are thought to be aligned ferromagnetically within the ab plane and antiferromagnetically between the adjacent planes.¹⁶ This spin structure can reconcile the FM correlation in the plane with the actual AF order at 56 K. At slightly above 50 K, the magnetic easy axis changes from the a to the b axis. At 48 K, $\chi(T)$ for all directions drastically decrease and become almost T independent. However, there is still substantial anisotropy with the same magnetic easy axis as in the high-temperature PM region, which is different from the one just above 48 K. This change implies that the spin structure is changed to another AF at 48 K.

The temperature dependence of C_p is shown in Fig. 3. As seen in other measurements, two transitions are clearly observed at 48 and 56 K. At the former one, C_p diverges dramatically, indicating that the first-order transition and the peak point is much higher than the values at room temperature. On the other hand, the latter one is a second-order AFM transition as discussed before. As shown in the inset of Fig. 3, the temperature dependence of C_p below 5 K behaves like $\gamma T + \beta T^3$. The estimated electronic specific-heat coefficient γ is 1.7 mJ/Ru mol K², which is more than about 10 times

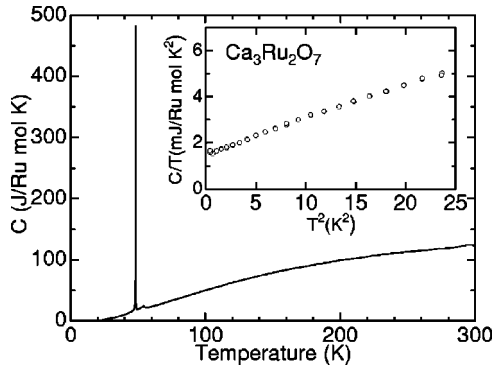


FIG. 3. The temperature dependence of the specific heat of $\text{Ca}_3\text{Ru}_2\text{O}_7$. The inset shows the plot of C/T vs T^2 below 5 K.

smaller than the previously reported values.^{14,16} The values of γ did not have any sample dependence. At room temperature, C_p almost saturates at 120 J/Ru mol K, close to the value of the Dulong-Petit's law (150 J/Ru mol K).

Figure 4(a) shows magnetization curves at various temperatures for both the increasing and decreasing fields along the a axis. Above 56 K, the magnetization curve shows linear (PM) characteristics. For $T < 56$ K, metamagnetic transitions emerge below 6 T. In the metallic AFM region ($48 < T < 56$ K), the transitions are broad, while steplike transitions are evident below 48 K. The transition field increases with decreasing temperature. The magnetizations above the transition field do not saturate up to 7 T, and they

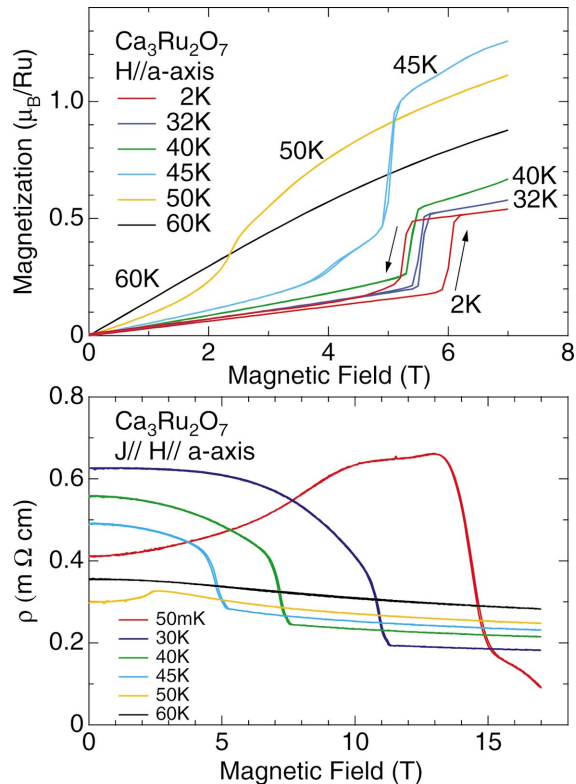


FIG. 4. (Color) (a) Magnetization curves $M(H)$ at various temperatures for the field along the a axis. (b) Field dependences of ρ_a at various temperatures for the field along the a axis in $\text{Ca}_3\text{Ru}_2\text{O}_7$.

exhibit a smaller moment in comparison with the full ($S = 1$) moment of $2\mu_B$. As for the anisotropy between the a and the b axis, the values of magnetization at 2 K after the transition are $0.5\mu_B$ for $H//a$ and $1.8\mu_B$ for $H//b$, respectively. In the magnetization curve at 45 K, multistep transitions are observed. Below 32 K, a metamagnetic transition with a hysteresis appears. At 2 K, the metamagnetic transition occurs at 5.9 T with increasing field, while at 5.3 T with decreasing field, as denoted by arrows in Fig. 4(a). The area of the hysteresis loop diminishes with increasing temperature and then a hysteresis disappears above 40 K.

Figure 4(b) shows the field dependences of ρ_a along the a axis at various temperatures. At 50 mK (i.e., in the metallic state of ρ_a), $\rho_a(H)$ gradually increases with increasing field (< 13.5 T) and then decreases sharply after the transition around 14 T. Surprisingly, no transition is observed around 6 T, where a metamagnetic transition is seen in the magnetization. On the other hand, $\rho_c(H)$ for the field along both the a and b axes show sudden drops around 6 T (not shown), which was discussed in Ref. 17 on the basis of a colossal magnetoresistance (CMR) and a tunneling magnetoresistance (TMR).^{17,18} The latter one is a tunneling effect facilitated by a field-induced coherent motion of spin-polarized metallic FM layers, which is often seen in a FM-insulator (I)-FM junction. In the present case, considering the layered structure of $\text{Ca}_3\text{Ru}_2\text{O}_7$, assuming that the RuO_2 layer is the metallic FM one, ρ_c corresponds to the case of a FM-I-FM junction, whereas ρ_a corresponds to the resistivity for the current along the metallic FM layer. In such a case, it is natural that ρ_a does not show any change around 6 T. Therefore, we can say that the lower field transition of $\rho_a(H)$ can be explained by a TMR. As for the higher field transition (at 14 T and 50 mK), the structural change is expected to play an important role. For $30 < T < 48$ K, ρ_a gradually decreases when the field is increased up to the transition, which is different behavior from that in the low- T metallic state. The transition field, corresponding to the higher field transition, decreases with increasing temperature. At 45 K, the transition around 5 T corresponds to the second transition in magnetization. These results strongly suggest that the magnetization along the a axis is expected to show a secondary metamagnetic transition at a higher field ($\mu_0 H > 7$ T) below 45 K and that this is the reason that the magnetic moment is significantly smaller than $2\mu_B$ from 2–40 K.

Taking account of the 2D metallic conduction, it is not unusual if quantum oscillations are observed for the field nearly along the c axis. Figure 5 shows ρ_c at 60 mK as a function of the inverse field for $H//c$ axis. In fact, periodical oscillations can be observed from 0.08 – 0.28 T^{-1} (i.e., $3.5 < \mu_0 H < 12.5$ T) without any metamagnetic transition, indicating the Shubnikov-de Haas oscillations. By executing a fast fourier transform (FFT) analysis, the estimated frequencies are 33.7 T and its harmonics, which are in reasonable agreement with the report of Cao *et al.*¹⁷ The obtained frequency corresponds to only 0.25% of the area of its first Brillouin zone.

Finally, let us discuss the ground state of $\text{Ca}_3\text{Ru}_2\text{O}_7$. A sudden decrease and the T -independent behavior of $\chi(T)$ at low temperature remind us of a spin-Peierls system¹⁹ or of

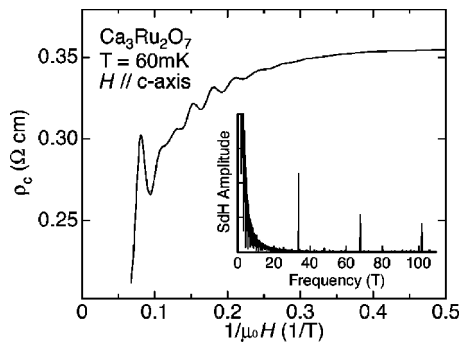


FIG. 5. The resistivity vs inverse field plot for the field and current along the c axis in $\text{Ca}_3\text{Ru}_2\text{O}_7$. The inset shows its FFT spectrum.

perovskite manganites, for example, $\text{Nd}_{0.45}\text{Sr}_{0.55}\text{MnO}_3$.²⁰ In particular, the latter one has a related crystal structure and has A -type AFM as a magnetic ground state. It shows structural change at T_N and CMR in a wide temperature range. From many similarities between manganites and $\text{Ca}_3\text{Ru}_2\text{O}_7$, the magnetic ground state may be conjectured to be A -type AFM, as pointed out in the latest report.¹⁶ However, considering the change of the anisotropy in $\chi(T)$ at two transition temperatures, it needs further studies to determine the exact spin structure. In the single-layered ruthenates, 2D transport properties indicate that d_{xy} orbital in t_{2g} , which can cause the FM instability, plays a crucial role in the metallic state.²¹ Although there can be a difference between the single and

the double layer, we assume that the same discussion for the d_{xy} orbital can be adopted. In the PM region, the positive Weiss temperatures indicate that the d_{xy} orbital plays the most important role in the transport and magnetic properties. However, the change of lattice parameters at 48 K may affect the energy-level scheme of t_{2g} orbitals. As a result, the contribution from d_{yz} and/or d_{zx} orbitals may become dominant instead of that from the d_{xy} orbital. There is a possibility that a small nested Fermi surface can be formed by the band from a d_{yz}/d_{zx} orbital having one-dimensional dispersion within the conducting plane, which may explain the 2D transport property with a small Fermi surface.

In conclusion, we summarize the features that are different from the previous reports. $\text{Ca}_3\text{Ru}_2\text{O}_7$ has a quasi-two-dimensional metallic ground state with a large anisotropy between ρ_{ab} and ρ_c . Quantum oscillations are observed in the 2D metallic state below 30 K. The temperature dependence of specific heat reveals that the electronic specific-heat coefficient γ is as small as 1.7 mJ/Ru mol K². A qualitative difference exists between the field dependences of ρ_{ab} and ρ_c . From the results of the field dependence of resistivity, we can explain the metamagnetic transition around 6 T on the basis of TMR.

The authors thank M. Ishikawa, Y. Uwatoko, E. Ohmichi, K. Yamaji, T. Yanagisawa, A. Iyo, S. Koikegami, and S. Hara for their help and comments. This study is supported by a domestic research fellowship from Japan Society for the Promotion of Science.

*Electronic address: yoshida.y@aist.go.jp

¹Y. Maeno, H. Hashimoto, K. Yoshida, S. Nishizaki, T. Fujita, J. Bednorz, and F. Lichtenberg, *Nature (London)* **372**, 534 (1994).
²Y. Maeno, T. M. Rice, and M. Sigrist, *Phys. Today* **54**, 42 (2001).
³K. Ishida, H. Mukuda, Y. Kitaoka, K. Asayama, Z. Q. Mao, Y. Mori, and Y. Maeno, *Nature (London)* **396**, 658 (1998).
⁴S. I. Ikeda, Y. Maeno, S. Nakatsuji, M. Kosaka, and Y. Uwatoko, *Phys. Rev. B* **62**, R6089 (2000).
⁵S. I. Ikeda, U. Azuma, N. Shirakawa, Y. Nishihara, and Y. Maeno, *J. Cryst. Growth* **237–239**, 787 (2002).
⁶S. Grigera, R. Perry, A. Schofield, M. Chiao, S. Julian, G. Lonzarich, S. Ikeda, Y. Maeno, A. Millis, and A. P. Mackenzie, *Science* **294**, 329 (2001).
⁷A. Callaghan, C. W. Moeller, and R. Ward, *Inorg. Chem.* **5**, 1572 (1966).
⁸T. Kiyama, K. Yoshimura, K. Kosuge, H. Michor, and G. Hilscher, *J. Phys. Soc. Jpn.* **67**, 307 (1998).
⁹S. Nakatsuji, S. I. Ikeda, and Y. Maeno, *J. Phys. Soc. Jpn.* **66**, 1868 (1997).
¹⁰C. S. Alexander, G. Cao, V. Dobrosavljevec, S. McCall, J. E. Crow, E. Lochner, and R. P. Guertin, *Phys. Rev. B* **60**, R8422 (1999).

¹¹F. Nakamura, T. Goko, M. Ito, T. Fujita, S. Nakatsuji, H. Fukazawa, Y. Maeno, P. Alireza, D. Forsythe, and S. Julian, *Phys. Rev. B* **65**, 220402 (2002).
¹²K. Yoshimura, T. Imai, T. Kiyama, K. R. Thurber, A. W. Hunt, and K. Kosuge, *Phys. Rev. Lett.* **83**, 4397 (1999).
¹³T. He and R. J. Cava, *Phys. Rev. B* **63**, 172403 (2001).
¹⁴G. Cao, S. McCall, J. E. Crow, and R. P. Guertin, *Phys. Rev. Lett.* **78**, 1751 (1997).
¹⁵G. Cao, K. Abboud, S. McCall, J. E. Crow, and R. P. Guertin, *Phys. Rev. B* **62**, 998 (2000).
¹⁶S. McCall, G. Cao, and J. E. Crow, *Phys. Rev. B* **67**, 094427 (2003).
¹⁷G. Cao, L. Balicas, Y. Xin, J. E. Crow, and C. S. Nelson, *Phys. Rev. B* **67**, 184405 (2003).
¹⁸E. Ohmichi, Y. Yoshida, S. I. Ikeda, N. Shirakawa, and T. Osada, (unpublished).
¹⁹M. Hase, I. Terasaki, and K. Uchinokura, *Phys. Rev. Lett.* **70**, 3651 (1993).
²⁰H. Kuwahara, T. Okuda, Y. Tomioka, A. Asamitsu, and Y. Tokura, *Phys. Rev. Lett.* **82**, 4316 (1999).
²¹Z. Fang and K. Terakura, *Phys. Rev. B* **64**, 020509 (2002).